

Nernst effect in the cuprate superconductor $\text{YBa}_2\text{Cu}_3\text{O}_y$: Broken rotational and translational symmetries

J. Chang,¹ Nicolas Doiron-Leyraud,¹ Francis Laliberté,¹ R. Daou,^{1,*} David LeBoeuf,^{1,†} B. J. Ramshaw,² Ruixing Liang,^{2,3} D. A. Bonn,^{2,3} W. N. Hardy,^{2,3} Cyril Proust,^{4,3} I. Sheikin,⁵ K. Behnia,⁶ and Louis Taillefer^{1,3,‡}

¹*Département de physique & RQMP, Université de Sherbrooke, Sherbrooke, Canada*

²*Department of Physics & Astronomy, University of British Columbia, Vancouver, Canada*

³*Canadian Institute for Advanced Research, Toronto, Canada*

⁴*Laboratoire National des Champs Magnétiques Intenses, UPR 3228 (CNRS, INSA, UJF, UPS), 31400 Toulouse, France*

⁵*Laboratoire National des Champs Magnétiques Intenses (CNRS), 38042 Grenoble, France*

⁶*LPEM (UPMC-CNRS), ESPCI, 75231 Paris, France*

(Dated: May 1, 2022)

The Nernst coefficient of the cuprate superconductor $\text{YBa}_2\text{Cu}_3\text{O}_y$ was recently shown to become strongly anisotropic within the basal plane when cooled below the pseudogap temperature T^* , revealing that the pseudogap phase breaks the four-fold rotational symmetry of the CuO_2 planes. Here we report on the evolution of this Nernst anisotropy at low temperature, once superconductivity is suppressed by a magnetic field. We find that the anisotropy drops rapidly below 80 K, to vanish in the $T = 0$ limit. We show that this loss of anisotropy is due to the emergence of a small high-mobility electron-like pocket in the Fermi surface at low temperature, a reconstruction attributed to a low-temperature state that breaks the translational symmetry of the CuO_2 planes. We discuss the sequence of broken symmetries – first rotational, then translational – in terms of an electronic nematic-to-smectic transition such as could arise when unidirectional spin or charge modulations order. We compare $\text{YBa}_2\text{Cu}_3\text{O}_y$ with iron-pnictide superconductors where the process of (unidirectional) antiferromagnetic ordering gives rises to the same sequence of broken symmetries.

PACS numbers: 74.25.Fy

I. INTRODUCTION

Establishing and understanding the normal-state phase diagram of cuprates is of primary importance in the quest to uncover the mechanism of high-temperature superconductivity. The discovery of quantum oscillations in underdoped $\text{YBa}_2\text{Cu}_3\text{O}_y$ (YBCO) revealed that in the absence of superconductivity, suppressed by application of a large magnetic field, the ground state in the underdoped region of the phase diagram is a metal whose Fermi surface contains a small closed pocket.¹ The negative Hall and Seebeck coefficients of YBCO at $T \rightarrow 0$ show this pocket to be electron-like.^{2,3} The presence of an electron pocket in the Fermi surface of a hole-doped cuprate is the typical signature of a Fermi-surface reconstruction caused by the onset of a new periodicity which breaks the translational symmetry of the crystal lattice.^{4,5}

In the doping phase diagram of YBCO (Fig. 1), the electron pocket exists at $T \rightarrow 0$ (in the absence of superconductivity) throughout the range from $p = 0.083$ to at least $p = 0.152$.⁸ We infer that translational symmetry is broken at $T = 0$ over at least that range, by an ordered phase that has yet to be definitively identified. The fact that the Seebeck coefficient of the cuprate $\text{La}_{1.8-x}\text{Sr}_x\text{Eu}_{0.2}\text{CuO}_4$ (Eu-LSCO) at $T \rightarrow 0$ is negative over the same range of doping as in YBCO,⁹ and that stripe order – a unidirectional modulation of spin and/or charge densities^{10,11} – prevails in Eu-LSCO over that doping range,¹² is compelling evidence that stripe order

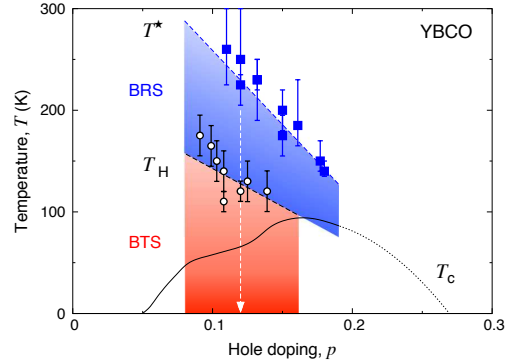


FIG. 1: Phase diagram of YBCO, showing the zero-field superconducting transition temperature T_c (dotted line, Ref. 6, extrapolated as dashed line above $p = 0.18$) and the pseudogap crossover temperature T^* detected by the Nernst effect (squares; Ref. 7). The onset of in-plane anisotropy in the Nernst coefficient below T^* shows that the pseudogap phase is a state with broken rotational symmetry (BRS).⁷ Once superconductivity is suppressed by a magnetic field, the normal state at $T \rightarrow 0$ is characterized by a reconstructed Fermi surface,^{1,2} evidence of broken translational symmetry (BTS). The temperature T_H below which the Hall coefficient $R_H(T)$ starts to deviate downward is the first signature of Fermi-surface reconstruction upon cooling (open circles; from Ref. 8). The white down-pointing arrow locates the present study of Nernst anisotropy on the phase diagram. The two dashed lines are a guide to the eye.

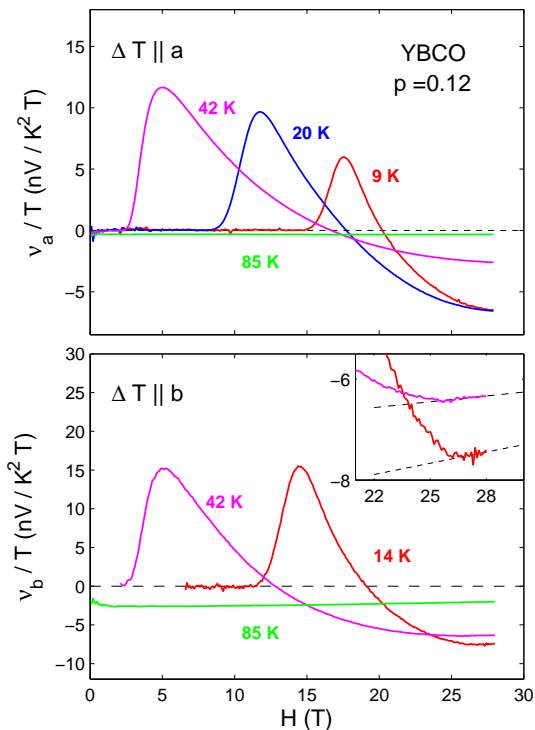


FIG. 2: Nernst coefficient ν of YBCO at a hole concentration (doping) $p = 0.12$, plotted as ν/T versus magnetic field H , for different temperatures, as indicated. Top: the temperature gradient ΔT is applied along the a axis of the orthorhombic crystal structure. Bottom: ΔT is along the b axis. Inset: zoom on the data at high field. The saturation in ν vs H above $H \simeq 26$ T indicates that the positive contribution from superconducting fluctuations has become negligible, and the data above 26 T represent the normal-state properties of YBCO at that doping.

is responsible for the broken translational symmetry and that Fermi-surface reconstruction is a generic property of hole-doped cuprates.

At temperatures above the superconducting transition temperature T_c , the normal-state phase diagram of cuprates is characterized by the pseudogap phase, below a crossover temperature T^* .¹³ The Nernst effect was recently found to be a sensitive probe of the pseudogap phase,^{7,14,15} such that it can be used to detect T^* , as shown in Fig. 1 for YBCO. Measurements of the Nernst coefficient $\nu(T)$ in detwinned crystals of YBCO for a temperature gradient along the a -axis and b -axis directions within the basal plane of the orthorhombic crystal structure revealed a strong in-plane anisotropy, setting in at T^* .⁷ This showed that the pseudogap phase breaks the four-fold rotational symmetry of the CuO_2 planes, throughout the doping range investigated, from $p = 0.08$ to $p = 0.18$.⁷

In this paper, we investigate the impact of Fermi-surface reconstruction on this Nernst anisotropy, by extending the previous Nernst study to low temperature. We find that below 80 K the anisotropy falls rapidly,

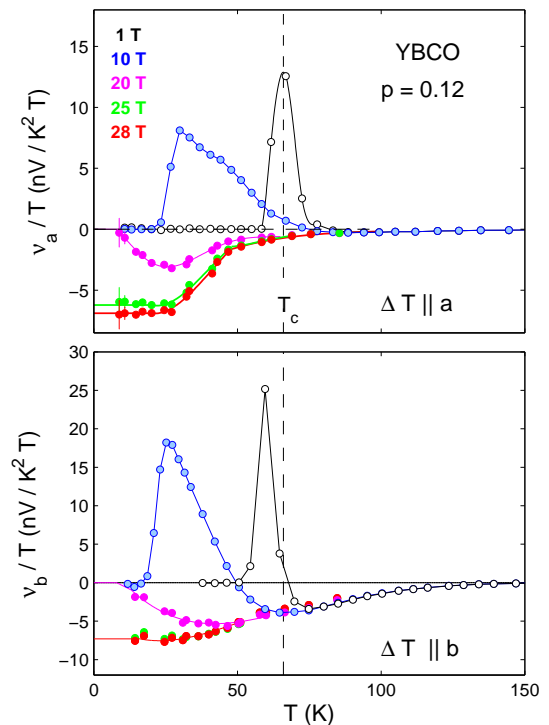


FIG. 3: Nernst coefficient ν of YBCO at $p = 0.12$, plotted as ν/T versus temperature T , for different values of the magnetic field, as indicated. Top: ΔT is along the a axis. Bottom: ΔT is along the b axis. The vertical dashed line marks the zero-field superconducting transition, at $T_c = 66.0$ K.

in close parallel with the fall in the Hall coefficient to negative values. We infer that the Nernst anisotropy disappears because the small closed high-mobility electron pocket which dominates the transport properties of YBCO at low temperature yields isotropic transport.

II. METHODS

Measurements were performed on high-quality detwinned YBCO crystals grown in a non-reactive BaZrO_3 crucible from high-purity starting materials.¹⁶ The oxygen content was set at $y = 6.67$ and the dopant oxygen atoms were made to order into an ortho-VIII superstructure, yielding a superconducting transition temperature $T_c = 66.0$ K. The hole concentration (doping) $p = 0.12$ was determined from a relationship between T_c and the c -axis lattice constant⁶.

The Nernst effect, being the transverse voltage V generated by a longitudinal temperature difference ΔT in a perpendicular applied magnetic field H ,^{17,18} was measured in Sherbrooke up to 15 T and at the LNCMI in Grenoble up to 28 T. In both cases, we used a one-heater two-thermometer setup and the field was applied along the c axis of the orthorhombic crystal structure. The Nernst signal was measured with the thermal gradient ΔT either along the a axis (ΔT_a) or the b axis (ΔT_b),

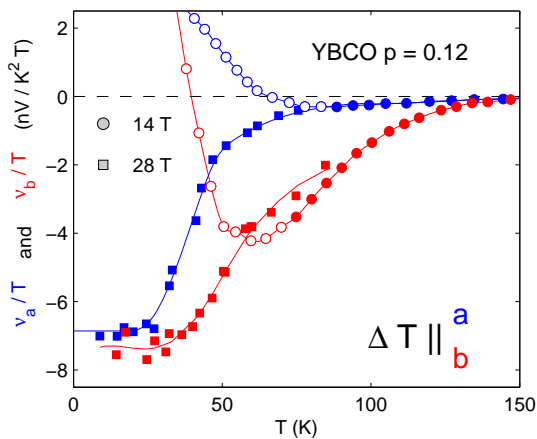


FIG. 4: Nernst coefficient ν of YBCO plotted as ν/T vs T for the two directions of temperature gradient (ν_a for $\Delta T \parallel a$, blue symbols; ν_b for $\Delta T \parallel b$; red symbols), for two values of the magnetic field: $H = 14$ T (circles) and 28 T (squares). Full symbols correspond to normal-state data, in which the superconducting contribution to the Nernst signal is negligible. Note that the normal-state data for ν_b at 14 T and 28 T do not quite coincide because of a slight field dependence of ν_b , akin to magnetoresistance (see isotherm at 85 K in Fig. 2).

and the Nernst coefficient ν is indexed as follows:

$$\nu_a = \frac{\alpha}{H} \frac{V_b}{\Delta T_a} \quad \text{and} \quad \nu_b = \frac{\alpha}{H} \frac{V_a}{\Delta T_b} \quad (1)$$

where $\alpha = \ell/w$ is the ratio of sample length (between thermometer contacts) to sample width.

III. RESULTS

Before we present our results, it is important to emphasize that there are two different contributions to the Nernst effect in a superconductor: 1) a positive contribution from superconductivity (moving vortices and fluctuations of the superconducting order parameter); 2) a contribution from normal-state quasi-particles, which can be either positive or negative. In YBCO, the two contributions can be readily separated because the quasi-particle contribution is negative, of opposite sign to the signal from superconducting fluctuations.⁷ Note also that the quasi-particle contribution to the Nernst coefficient $\nu(H)$ is mostly independent of field, whereas the superconducting contribution is strongly dependent on field.¹⁷ In the electron-doped cuprate $\text{Pr}_{2-x}\text{Ce}_x\text{CuO}_4$, for example, this difference in the field dependence was used to separate the two contributions, both positive in this case.¹⁹

The amplitude of the quasi-particle contribution may be estimated from the following expression:¹⁸

$$\left| \frac{\nu}{T} \right| \simeq \frac{\pi^2}{3} \frac{k_B}{e} \frac{\mu}{T_F} \quad (2)$$

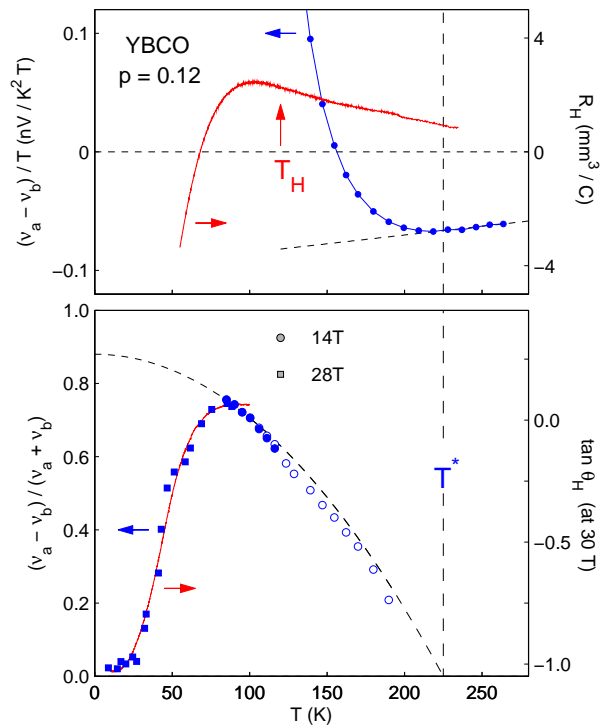


FIG. 5: Temperature dependence of the in-plane anisotropy in the normal-state Nernst coefficient of YBCO at $p = 0.12$. Top: Nernst anisotropy difference $(\nu_a - \nu_b)/T$ vs T (blue circles, left axis; from Ref. 7). The difference starts to rise below the pseudogap temperature T^* (vertical dashed line). Also shown is the Hall coefficient $R_H(T)$, measured in a field $H = 10$ T (continuous red curve, right axis). Below ~ 100 K, $R_H(T)$ drops precipitously to reach large negative values at $T \rightarrow 0$.^{2,8} We can define the onset of this drop as T_H , the temperature below which $R_H(T)$ acquires downward curvature (see Ref. 8). Bottom: Normalized Nernst anisotropy defined as the dimensionless ratio $(\nu_a - \nu_b)/(\nu_a + \nu_b)$, plotted vs T below 120 K (full blue symbols; squares, $H = 28$ T, this work; circles, $H = 14$ T, from Ref. 7). (Because both $\nu_a(T)$ and $\nu_b(T)$ cross zero around 150 K, the ratio becomes ill-defined above 120 K. To avoid this, we define the sum and difference relative to their value at T^* and plot their ratio above 120 K (open blue circles); see Ref. 7.) Below ~ 80 K, the anisotropy ratio drops rapidly to zero as $T \rightarrow 0$ in a way that precisely tracks the drop in the Hall coefficient, shown here as $\tan \theta_H(T) \equiv \rho_{xy}/\rho_{xx}$ vs T (continuous red curve, right axis), where the transverse (ρ_{xy}) and longitudinal (ρ_{xx}) resistivities are measured in 30 T. This reveals that the disappearance of the Nernst anisotropy at low temperature is due to the Fermi-surface reconstruction that leads to the formation of a small closed electron pocket of high mobility (see text).

where k_B is Boltzmann's constant, e is the electron charge, μ is the carrier mobility and T_F the Fermi temperature. This relation, applicable in the $T \rightarrow 0$ limit, was found valid within a factor of two for a wide range of metals.¹⁸ Its implication is that the Nernst effect is highly sensitive to Fermi-surface reconstructions that produce pockets with a small Fermi energy ($\epsilon_F \equiv k_B T_F$) and

a high mobility. A good example of this is the heavy-fermion metal URu₂Si₂ where, upon cooling below 17 K, ϵ_F drops by a factor of ten simultaneously with a ten-fold rise in the mobility μ . As a consequence, ν/T rises by two orders of magnitude.²⁰

In Figs. 2 and 3, the Nernst coefficient ν of YBCO at $p = 0.12$ is plotted as ν/T vs H and vs T , respectively, for both a - and b -axis directions. The high-field b -axis data are presented here for the first time, while the low-field data⁷ and the high-field a -axis data³ were reported previously. We start by examining the isotherms (Fig. 2). At $T < T_c = 66$ K, $\nu(H)$ shows the strong field dependence typical of a superconductor: 1) at low field, $\nu = 0$ in the vortex solid phase; 2) at intermediate fields, ν rises to give a strong positive peak; 3) at higher field, the positive signal gradually decreases, until such fields as $\nu(H)$ becomes flat, where the superconducting contribution has become negligible. At the highest field measured in our experiment, 28 T, this saturation has been reached for all temperatures down to ~ 10 K, so that we may regard the state at 28 T (and above) as the normal state.

At $T = 85$ K, $\nu_a(H)$ is seen to be totally flat and $\nu_b(H)$ increases very slightly (a form of normal-state magneto-resistance). The positive (field-decreasing) superconducting contribution has become vanishingly small. This shows that in a clean underdoped cuprate the regime of significant superconducting fluctuations does not extend in temperature very far beyond T_c . More quantitatively, the superconducting contribution to the Nernst coefficient ν/T in YBCO drops to 0.1% of its peak value at T_c by $T \simeq 1.35 T_c$.

In Fig. 3, we see that the normal-state ν/T at 28 T is independent of temperature below ~ 25 K. Its large negative value at $T \rightarrow 0$ is completely and unambiguously due to quasi-particles. In Fig. 4, we compare the normal-state ν_a and ν_b as a function of temperature. We see that the large anisotropy characteristic of the pseudogap phase disappears below ~ 25 K.

The in-plane anisotropy of the normal-state $\nu(T)$ is plotted in Fig. 5, as the difference $\nu_a/T - \nu_b/T$ (top panel) and the normalized difference $(\nu_a - \nu_b)/(\nu_a + \nu_b)$ (bottom panel). The Nernst anisotropy is seen to rise just below the pseudogap temperature T^* , defined as the temperature below which the a -axis resistivity drops below its linear dependence at high temperature.⁷ Upon cooling, it continues to rise, until it reaches a maximal value of $(\nu_a - \nu_b)/(\nu_a + \nu_b) \simeq 0.75$ (*i.e.* $\nu_a/\nu_b \simeq 7$) at ~ 80 K. Upon further cooling, however, we now find that the anisotropy drops rapidly, with $(\nu_a - \nu_b)/(\nu_a + \nu_b) \rightarrow 0$ (*i.e.* $\nu_a/\nu_b \rightarrow 1$) as $T \rightarrow 0$.

IV. DISCUSSION

To elucidate the cause of this dramatic drop in the Nernst anisotropy, we turn to the Hall coefficient $R_H(T)$. In Fig. 5, the normal-state Hall angle θ_H is plotted

as $\tan \theta_H = \rho_{xy}/\rho_{xx}$, the ratio of Hall to longitudinal resistivities. Upon cooling, we see that the drop in $\tan \theta_H(T)$ to negative values tracks precisely the drop in Nernst anisotropy. (Note that from the Onsager relation, $\sigma_{xy} = -\sigma_{yx}$, R_H is independent of current direction in the basal plane.²¹)

A. Fermi-surface reconstruction

1. Electron pocket

Soon after the discovery of quantum oscillations in YBCO,¹ the fact that the oscillations were seen on top of a large background of negative Hall resistance led to the interpretation that the oscillations come from orbits around an electron-like Fermi pocket.² This interpretation was later confirmed by the observation of a large negative Seebeck coefficient at low temperature.³ Clinching evidence came recently from the quantitative agreement between the measured (negative) value of S/T at $T \rightarrow 0$, on the one hand, and the magnitude of S/T expected from the Fermi energy inscribed in the quantum oscillations, on the other hand, both obtained in YBCO at the same doping, namely $p = 0.11$.⁹ Therefore, in the doping interval from $p = 0.083$ to at least $p = 0.152$,^{8,9} the Fermi surface of YBCO in its non-superconducting ground state contains a small closed electron pocket. This pocket dominates the transport properties at low temperature, as discussed in detail in Ref. 8. In particular, it produces a large (quasiparticle) Nernst signal. Applying Eq. 1 to YBCO at $p = 0.11$, where quantum oscillations give $T_F = 410 \pm 20$ K and $\mu = 0.02 \pm 0.006$ T⁻¹,²² yields $|\nu/T| = 13 \pm 3$ nV/K²T, while the measured value at $p = 0.11$ is $\nu/T = -13 \pm 3$ nV/K²T,⁹ in perfect agreement. The somewhat smaller value at $p = 0.12$, namely $\nu/T \simeq -7$ nV/K²T as $T \rightarrow 0$ (Fig. 4), is probably due to the lower mobility expected of samples in the ortho-VIII phase (with $y = 6.67$) compared to those in the ortho-II phase (with $y = 6.54$), consistent with the much weaker quantum oscillations in the former.

The fact that $\nu_a \simeq \nu_b$ as $T \rightarrow 0$ shows that the electron pocket yields transport properties that are isotropic in the plane. This explains two features of the transport in YBCO. The first is the jump in the in-plane anisotropy of the resistivity as the doping drops below $p = 0.08$.^{23,24} Indeed, it was recently discovered that the electron pocket disappears suddenly as the doping is reduced below a critical value $p = 0.08$,⁸ in the sense that for $p < 0.08$ both Hall⁸ and Seebeck⁹ coefficients depend weakly on temperature and remain positive at $T \rightarrow 0$. This change in Fermi-surface topology (or Lifshitz transition) coincides with a ten-fold increase in resistivity at $T \rightarrow 0$,⁸ showing that the high-conductivity part of the Fermi surface has disappeared. Once the high-mobility electron pocket is removed, the in-plane anisotropy ratio ρ_a/ρ_b rises (see Ref. 8).

The second feature is the rapid loss of in-plane

anisotropy in the Nernst coefficient upon cooling. As shown in Fig. 5, the precipitous drop in the anisotropy ratio $(\nu_a - \nu_b)/(\nu_a + \nu_b)$ below 80 K tracks closely the fall in the Hall signal (plotted as $\tan \theta_H$) towards large negative values. As the electron pocket becomes increasingly dominant upon cooling, *i.e.* as its mobility $\mu \propto \tan \theta_H$ increases, the Nernst signal becomes increasingly isotropic.

2. Stripe order

The natural explanation for the emergence of an electron pocket in a hole-doped cuprate is the onset of a new periodicity that breaks the translational symmetry of the lattice and thus reduces the Brillouin zone, causing a reconstruction of the large hole Fermi surface into smaller pieces.⁵ A recent study that compares YBCO to the hole-doped cuprate Eu-LSCO found that the Seebeck coefficient behaves in essentially identical fashion in the two materials, as a function of both temperature and doping:⁹ S/T drops to negative values (of very similar magnitude) below the same peak temperature, the sign-change temperature T_0^S is maximal at $p = 1/8$ in both cases, the drop in S/T disappears below the same critical doping $p = 0.08$. So the same Fermi-surface reconstruction must be taking place in Eu-LSCO as in YBCO, pointing to a generic mechanism of hole-doped cuprates.

Now in Eu-LSCO, charge modulations are observed by x-ray diffraction at low temperature,¹² over the entire doping range where $S/T < 0$.⁹ Spin modulations are most likely also present, as observed in the closely related material $\text{La}_{1.6-x}\text{Sr}_x\text{Nd}_{0.4}\text{CuO}_4$ (Nd-LSCO).²⁵ Called ‘stripe order’, these spin and charge modulations break the translational symmetry of the CuO_2 planes, and so will cause a reconstruction of the Fermi surface. Calculations for stripe order at $p = 1/8$ show that an electron pocket will generically appear,²⁶ causing the quasiparticle Nernst signal to be strongly enhanced.²⁷ It is then reasonable to infer that stripe order causes the Fermi-surface reconstruction in these underdoped cuprates.

Because stripe order involves unidirectional spin and/or charge modulations, it also breaks the four-fold rotational symmetry of the CuO_2 planes.^{10,11} So the reconstructed Fermi surface is expected to have strong in-plane anisotropy, manifest in the calculations by the presence of quasi-1D open sheets.²⁶ However, if the conductivity of the relatively isotropic electron pockets is much higher, at low temperature, than that of these open sheets, the inherent anisotropy of the latter will only show up in transport when the electron pocket disappears, as it does below $p = 0.08$.

B. The pseudogap phase

We have focused so far on the non-superconducting ground state at $T \rightarrow 0$, with its stripe order and recon-

structed Fermi surface. Let us now ask what happens when the temperature is raised.

The presence of the electron pocket persists at least as long as the Hall coefficient is negative. In YBCO at $p = 0.12$, $R_H(T)$ changes from negative to positive at the sign-change temperature $T_0^H = 70$ K, above $T_c = 66$ K.^{2,8} Of course, the drop in $R_H(T)$ starts at higher temperature, namely at the peak in $R_H(T)$ near 90 K (see Fig. 5). In fact, the onset of the downturn is really at the temperature T_H where the curvature changes from upward at high temperature to downward at low temperature, *i.e.* at the inflexion point. At $p = 0.12$, $T_H \simeq 120$ K (see Fig. 5). In Fig. 1, this temperature T_H is plotted vs p on the phase diagram of YBCO. We see that it lies inside the pseudogap phase, between the crossover temperature T^* and the zero-field superconducting temperature T_c . This means that the electron pocket starts emerging at temperatures well above the onset of superconductivity, and it does so even in small magnetic fields. In this sense, the onset of Fermi-surface reconstruction is not field-induced; it is a property of the zero-field pseudogap phase.

If T_H marks the onset of Fermi-surface reconstruction in YBCO as detected in the Hall effect, what corresponding characteristic temperature do we obtain from other transport properties? From the Seebeck coefficient S/T vs T , a similar characteristic temperature is obtained, with $T_S \simeq 100$ K at $p = 0.12$.^{3,9} However, the Nernst coefficient, plotted as ν/T vs T , starts its drop to large negative values at a temperature T_ν which is significantly higher, namely $T_\nu \simeq 225$ K at $p = 0.12$.⁷ (T_ν is independent of direction, the same whether it is measured in ν_a or ν_b .⁷) Calculations show that the quasiparticle Nernst effect is an extremely sensitive probe of Fermi-surface distortions such as would arise from broken rotational symmetry.²⁸ The value of T_ν is plotted as a function of doping in the phase diagram of Fig. 1. We see that $T_\nu \simeq 2 T_H$. Now T_ν coincides with the temperature T_ρ below which the in-plane (a -axis) resistivity $\rho_a(T)$ of YBCO deviates from its linear temperature dependence at high temperature. This T_ρ is regarded as the standard definition of the pseudogap crossover temperature T^* .²⁹ The fact that $T_\nu = T_\rho$ at all dopings shows that the drop in ν/T to negative values is a property of the pseudogap phase.

Given that the large value of ν/T at $T \rightarrow 0$ is firmly associated with the small high-mobility electron pocket in YBCO, can T_ν therefore be regarded as the onset of Fermi-surface reconstruction as detected in the Nernst effect? By the same token, can T_ρ be regarded as the onset of incipient Fermi-surface reconstruction detected in the resistivity? If so, then the pseudogap phase would be the high-temperature precursor of the stripe-ordered phase present at low temperature.

One evidence in support of a stripe-precursor scenario is the fact that the enhancement of the Nernst coefficient ν/T below T^* is anisotropic, that it breaks the rotational symmetry of the CuO_2 planes. This, of course, is a characteristic signature of stripe ordering. Indeed,

the sequence of broken symmetries, first rotational then translational, is expected in the gradual process of stripe ordering.³⁰ The sequence is called ‘nematic to smectic’ ordering. The fact that T_ν and T_ρ are higher than T_S and T_H , by roughly a factor 2, may come from the role of scattering in the various transport coefficients. Indeed, while ν and ρ both depend directly on the scattering rate (or mobility μ), with $\nu \propto \mu$ and $\rho \propto 1/\mu$, S and R_H do not (at least in a single band model). In other words, if stripe fluctuations affect the transport primarily through the scattering rate, then we would expect ρ and ν to be sensitive to the onset of stripe fluctuations, but not S and R_H . As we shall now see, similar precursor effects are observed in the iron-pnictide superconductors.

C. Comparison with pnictide superconductors

It is instructive to compare the cuprate superconductor YBCO with the iron-pnictide superconductor $\text{Ba}(\text{Fe}_{1-x}\text{Co}_x)_2\text{As}_2$ (Co-Ba122). In the parent compound BaFe_2As_2 , a well-defined antiferromagnetic order sets in below a critical temperature $T_N = 140$ K.³¹ This order is unidirectional, with chains of ferromagnetically aligned spins along the b -axis of the orthorhombic crystal structure alternating antiferromagnetically in the perpendicular direction (a -axis). In other words, this is a form of ‘spin-stripe’ order, which breaks both the translational and rotational symmetry of the original tetragonal lattice (present well above T_N). As Co is introduced, T_N falls, and superconductivity appears, with T_c peaking at the point where it crosses T_N . In other words, in the underdoped region the normal state is characterized by spin-stripe order for some range of temperature above T_c . This order causes a reconstruction of the Fermi surface, which leads to a change in the in-plane resistivity: a drop below T_N at low Co concentration x , an upturn at intermediate x . However, the upturn starts well above T_N . One can define a temperature T_ρ below which the roughly linear T dependence at high temperature turns upwards. For $3\% < x < 5\%$, $T_\rho \simeq 2 T_N$.³² Moreover, the rise in ρ is anisotropic: a strong in-plane anisotropy appears at T_ρ .³² At higher doping, above the quantum critical point where antiferromagnetic order disappears (in the absence of superconductivity), both the upturn and the anisotropy in ρ vanish.³²

The overall phenomenology is seen to be remarkably similar to that of YBCO. The unidirectional order that breaks translational symmetry and reconstructs the Fermi surface at low temperature is preceded at high temperature by a regime with strong in-plane transport anisotropy, evidence of broken rotational symmetry. In Co-Ba122, it is very natural to view this regime as the nematic precursor to the smectic phase at low temperature. The analogy supports the view that the pseudogap phase in YBCO is just such a precursor to stripe order.

It is interesting to note that in Co-Ba122 the in-plane anisotropy in ρ is not largest at $x = 0$, where the order

is strongest (T_N is highest). Indeed, the ratio ρ_b/ρ_a at $T \rightarrow 0$ is larger at $x > 2\%$ than at $x = 0$.³² This could well be due to a short-circuiting effect similar to that observed in YBCO, whereby a small and isotropic Fermi pocket of high mobility dominates the conductivity. Indeed, the concentration $x \simeq 0.02$ in Co-Ba122 appears to be a Lifshitz critical point, as suggested by ARPES experiments that reveal the existence of a small hole pocket for $x < 0.02$, and not above.³³ Such a pocket could short-circuit the in-plane anisotropy coming from other parts of the Fermi surface.

V. CONCLUSION

In summary, the Nernst effect is a highly sensitive probe of electronic transformations in metals. In the cuprate superconductor YBCO, the onset of the pseudogap phase at T^* causes a 100-fold enhancement of the quasiparticle Nernst coefficient, which goes smoothly from $\nu_b/T = +0.07$ nV/K²T at T^* to $\nu_b/T = -7$ nV/K²T at $T \rightarrow 0$, in the normal (non-superconducting) state. This enhancement is strongly anisotropic in the plane, showing that the pseudogap phase breaks the rotational symmetry of the CuO_2 planes. When the Fermi-surface reconstructs at low temperature, the formation of a high-mobility electron pocket short-circuits this in-plane anisotropy. The magnitude of ν/T at $T \rightarrow 0$ is in perfect agreement with the value expected from the small closed Fermi pocket detected in quantum oscillations. The negative sign proves that the signal comes from quasiparticles and not superconducting fluctuations or vortices. There is compelling evidence that the Fermi-surface reconstruction is caused by a stripe order which breaks the translational symmetry of the CuO_2 planes at low temperature,⁹ but also its rotational symmetry. The sequence of broken symmetries upon cooling, first rotational then translational, suggests a process of nematic-to-smectic stripe ordering, similar to that observed in the iron-pnictide superconductor Co-Ba122, where a phase of spin-stripe antiferromagnetic order prevails in the underdoped region of the temperature-concentration phase diagram. The analogy suggests that the enigmatic pseudogap phase of hole-doped cuprates is also a high-temperature precursor of a stripe-ordered phase, with unidirectional charge and/or spin modulations. This nematic interpretation is consistent with the in-plane anisotropy of the spin fluctuation spectrum detected by neutron scattering in underdoped YBCO.³⁴

VI. ACKNOWLEDGEMENTS

We thank J. Corbin and J. Flouquet for assistance with measurements in Sherbrooke and at the LNCMI in Grenoble, respectively. J.C. was supported by Fellowships from the Swiss SNF and FQRNT. Part of this work was supported by Euromagnet under the EU con-

tract RII3-CT-2004-506239. C.P. and K.B. acknowledge support from the ANR project DELICE. L.T. acknowledges support from the Canadian Institute for Advanced

Research, a Canada Research Chair, NSERC, CFI and FQRNT.

-
- * Present address: Max Planck Institute for Chemical Physics of Solids, Dresden 01187, Germany.
- † Present address: Laboratoire National des Champs Magnétiques Intenses, UPR 3228 (CNRS, INSA, UJF, UPS), Toulouse 31400, France.
- ‡ E-mail: louis.taillefer@physique.usherbrooke.ca.
- ¹ N. Doiron-Leyraud *et al.*, *Nature* **447**, 565 (2007).
 - ² D. LeBoeuf *et al.*, *Nature* **450**, 533 (2007).
 - ³ J. Chang *et al.*, *Phys. Rev. Lett.* **104**, 057005 (2010).
 - ⁴ L. Taillefer, *J. Phys.: Condens. Matter* **21**, 164212 (2009).
 - ⁵ S. Chakravarty, *Science* **319**, 735 (2008).
 - ⁶ R. Liang *et al.*, *Phys. Rev. B* **73**, 180505 (2006).
 - ⁷ R. Daou *et al.*, *Nature* **463**, 519 (2010).
 - ⁸ D. LeBoeuf *et al.*, *Phys. Rev. B* **83**, 054506 (2011).
 - ⁹ F. Laliberté *et al.*, arXiv:1102.0984.
 - ¹⁰ S.A. Kivelson *et al.*, *Rev. Mod. Phys.* **75**, 1201 (2003).
 - ¹¹ M. Vojta, *Adv. Phys.* **58**, 699 (2009).
 - ¹² J. Fink *et al.*, arXiv:1011.5101.
 - ¹³ M.R. Norman *et al.*, *Adv. Phys.* **54**, 715 (2005).
 - ¹⁴ O. Cyr-Choinière *et al.*, *Nature* **458**, 743 (2009).
 - ¹⁵ M. Matusiak *et al.*, *Europhys. Lett.* **86**, 17005 (2009).
 - ¹⁶ R. Liang *et al.*, *Physica C* **336**, 57 (2000).
 - ¹⁷ Y. Wang, L. Li, and N. P. Ong, *Phys. Rev. B* **73**, 024510 (2006).
 - ¹⁸ K. Behnia, *J. Phys.: Condens. Matter* **21**, 113101 (2009).
 - ¹⁹ P. Li and R.L. Greene, *Phys. Rev. B* **76**, 174512 (2007).
 - ²⁰ R. Bel *et al.*, *Phys. Rev. B* **70**, 220501 (2004).
 - ²¹ K. Segawa and Y. Ando, *Phys. Rev. B* **69**, 104521 (2004).
 - ²² C. Jaudet *et al.*, *Phys. Rev. Lett.* **100**, 187005 (2008).
 - ²³ Y. Ando *et al.*, *Phys. Rev. Lett.* **88**, 137005 (2002).
 - ²⁴ X. F. Sun, K. Segawa, and Y. Ando, *Phys. Rev. Lett.* **93**, 107001 (2004).
 - ²⁵ N. Ichikawa *et al.*, *Phys. Rev. Lett.* **85**, 1738 (2000).
 - ²⁶ A.J. Millis and M.R. Norman, *Phys. Rev. B* **76**, 220503 (2007).
 - ²⁷ A. Hackl, M. Vojta and S. Sachdev, *Phys. Rev. B* **81**, 045102 (2010).
 - ²⁸ A. Hackl and M. Vojta, *Phys. Rev. B* **80**, 220514 (2009).
 - ²⁹ T. Ito, K. Takenaka and S. Uchida, *Phys. Rev. Lett.* **70**, 3995 (1993).
 - ³⁰ S.A. Kivelson, E. Fradkin and V. J. Emery, *Nature* **393**, 550 (1998).
 - ³¹ P.C. Canfield and S.L. Budko, *Annu. Rev. Condens. Matter Phys.* **1**, 27 (2010).
 - ³² J.-H. Chu *et al.*, *Science* **324**, 329 (2010).
 - ³³ C. Liu *et al.*, *Nat. Phys.* **6**, 419 (2010).
 - ³⁴ V. Hinkov *et al.*, *Science* **319**, 597 (2008).